

An observational study of multiple tropical cyclone events in the western north Pacific

By KYLE D. KROUSE^{1*} and ADAM H. SOBEL², ¹*Department of Applied Physics and Applied Mathematics, Columbia University, New York, NY 10027, USA;* ²*Department of Applied Physics and Applied Mathematics and Department of Earth and Environmental Sciences, Columbia University, New York, USA*

(Manuscript received 26 May 2009; in final form 13 January 2010)

ABSTRACT

Best-track and NCEP/NCAR reanalysis data are used to study the statistics of multiple cyclone events (MCEs), in which one tropical cyclone (the ‘daughter’) forms to the east of another extant TC (the ‘mother’) during the mother’s lifetime, in the western north Pacific. It is found that approximately 30% of all tropical cyclones become mothers, and that MCEs occur relatively more frequently in the early and late season than the peak season. Composite differences in large-scale conditions between MCEs and events in which a daughter does not form show that MCEs are favoured by easterly vertical shear and cyclonic low-level horizontal shear. These findings are broadly consistent with (though they do not prove) the hypothesis that Rossby wave radiation is an important mechanism in a significant fraction of MCE events and that the radiation is governed by linear stationary wave dynamics.

1. Introduction

Due to the large-scale planetary vorticity gradient, tropical cyclones (TCs) sometimes radiate Rossby waves into the local atmospheric flow (Shapiro and Ooyama, 1990; Ferreira and Schubert, 1997). Cyclonic disturbances embedded in these wave trains can in some cases be the sites of new tropical cyclogenesis (Frank, 1982; Davidson and Hendon, 1989; Carr and Elsberry, 1995; Holland, 1995; Briegel and Frank, 1997; Ritchie and Holland, 1999; Li et al., 2003; Li and Fu, 2006; Fu et al., 2007) to the east of the original TC. We define a ‘multiple cyclone event’ (MCE) as an event in which a new tropical cyclone (the ‘daughter’) forms to the east of another extant TC (the ‘mother’) during the mother’s lifetime. In this paper, we study the statistics of MCEs as evident in the best track tropical cyclone database. Our purposes are to document some basic features of those statistics, and to document the large-scale conditions under which MCEs occur, compared to those under which they do not. The results are compared to hypotheses which are derived from the idealized modelling study of Krouse et al. (2008).

A number of previous studies have examined the idea that a TC can be a source of Rossby waves, and that those waves can provide the necessary atmospheric conditions for subsequent genesis of another TC. Davidson and Hendon (1989)

used ECMWF analysis data for the FGGE/WMONEX Southern Hemisphere summer (1978/79) to demonstrate the presence of a ‘downstream development’ mechanism over northern Australia. Some of the resulting cyclonic anomalies strengthened and developed into TCs. In their modelling studies, Carr and Elsberry (1995) demonstrated the occurrence of energy dispersion from an extant vortex. The dispersion is generally manifested as a Rossby wave train to the southeast of the first TC, which corresponds to the wake region of westward/northwestward-moving TCs. Analyzing 8 yr of data from the Australian Bureau of Meteorology, Ritchie and Holland (1999) identified 8% of the genesis cases as resulting from the eastward energy dispersion mechanism. Li et al. (2003) examined a particularly clear event during the 2000 season in the western north Pacific (WNP) which meets the criteria Ritchie and Holland (1999) used in identifying such an event. Li and Fu (2006) and Fu et al. (2007) expanded their satellite data analysis techniques to the entire WNP basin for the typhoon seasons of 2000 and 2001 and the genesis of six of the seasons’ 34 TCs ($\cong 18\%$), they determined, were due to the energy dispersion mechanism from an extant TC. We compute the fraction of MCEs over a larger data record and apply somewhat different criteria than these previous studies. We also compute a number of statistics aimed at discriminating the different large-scale conditions under which MCEs occur from those under which only single TCs do.

One aim of these calculations is to determine whether the observations can falsify the hypothesis that the ideas of Krouse et al. (2008) are relevant to typical MCEs in observations. Krouse et al.

*Corresponding author.

e-mail: kdk8@columbia.edu

DOI: 10.1111/j.1600-0870.2010.00435.x

(2008) modelled the wave radiation process using the shallow water equations on the sphere, representing the TC by a forced vortex generated by a localized mass sink which translated in longitude at a specified velocity. This mass sink was imposed on a fluid layer otherwise at rest. We found that wave trains qualitatively resembling those observed would only form when the mass sink was translated westward. This result is easily understood using linear Rossby wave dynamics in the shallow-water system. Stationary Rossby wave solutions are only possible in the presence of an eastward background flow. The simulated long-lived wave trains were stationary in the comoving frame of the imposed vortex, and in that frame the background flow is eastward for a vortex moving westward, since the ambient fluid in the far field is at rest in the relevant resting frame (i.e. that rotating with the planet). The wavelength of the radiated waves was also found to depend on the magnitude of the vortex translation speed, a dependence consistent with that obtained from assuming stationary linear Rossby wave solutions.

The application of these ideas to observed disturbances is more complex. The key quantity is the large-scale environmental steering flow felt by the radiated Rossby waves, evaluated in the frame comoving with the vortex. As a real TC's motion is, to first order, also determined by advection by an appropriately defined steering flow, we need to determine the difference between that steering flow and the one that is felt by the waves. Existing literature suggests that at least in many cases the steering of a TC will be more strongly influenced by the upper level flow than will the steering of typical short Rossby waves (sometimes called 'easterly waves' or 'tropical depression type disturbances') found in the tropics. This implies that when the vertical shear of the zonal flow is easterly ($\frac{\partial u}{\partial z} < 0$), the TC will be advected westward more strongly than the waves, so that the steering flow felt by the waves in the TC frame will be eastward. In this case we expect wave radiation to occur. Westerly shear implies that the waves feel westward environmental flow in the TC frame, and in this case we do not expect wave radiation.

Although not discussed by Krouse et al. (2008), easterly shear also tends to inhibit vertical propagation of Rossby waves. For this reason as well, we might expect that an easterly sheared environment would tend to support stronger wave radiation at low levels, by preventing the escape of wave activity to the upper troposphere. Recent theoretical and numerical studies further support this idea. Wang and Xie (1996) and Ge et al. (2007) find that an easterly vertical shear tends to greatly enhance the amplitude of the TD-type waves at the lower levels and that the energy dispersion-induced equatorial Rossby wave train is strengthened as well.

The ideas of Krouse et al. (2008) can also be interpreted in terms of horizontal shear. Since the Rossby wave trains tend to be emitted towards the equator as well as eastward, a large-scale cyclonic flow is associated with eastward steering of the waves in the TC frame. We thus expect wave radiation in cyclonic horizontal shear but not in anticyclonic shear.

Both the vertical and horizontal shear arguments predict not only under which conditions wave radiation can occur, but, through the Rossby wave dispersion relation, that the wavelength of the waves will increase with the magnitude of the shear if the sign of the shear is favourable for radiation. The prediction is easily made quantitative in the shallow water context (as in Krouse et al. (2008)) but it is somewhat more difficult to do so in the fully stratified system, due to the difficulty of defining the steering level precisely.

In this paper we use observations of MCEs to test these predictions. We use MCEs as indicators of Rossby wave radiation, and compare the conditions under which MCEs do or do not occur in the observations to those under which we expect wave radiation to occur or not, according to the linear wave ideas discussed above. If a second TC (the 'daughter') forms to the east of a pre-existing one (the 'mother') within the lifetime of the mother, a plausible hypothesis is that the genesis of the daughter was preconditioned by a synoptic-scale cyclonic disturbance generated by Rossby wave radiation from the mother. Other causalities are of course possible; both TCs could have resulted from disturbances that coevolved as part of a synoptic-scale wave train which itself developed for reasons other than downstream development, or the second one could have evolved for reasons entirely unrelated to the first one. Another possible scenario is that the multiple cyclones are formed via the ITCZ breakdown mechanism as they are occasionally in the eastern Atlantic and eastern Pacific (Schubert et al., 1991; Molinari et al., 1997; Ferreira and Schubert, 1997; Dickinson and Molinari, 2000; Wang and Magnusdottir, 2005, 2006). To the best of the authors' knowledge, however, there exists no documentation of this occurring in the WNP (see, for example, the discussion in Sobel and Bretherton, 1999). Yet another possibility (Dunkerton and Baldwin, 1995; Fu et al., 2007) is that the upper-level divergence stimulates Rossby waves which are then ducted to lower levels and pushed to the south east by the lower-level monsoon westerlies. These waves may then subsequently develop into disturbances themselves oriented in a manner that would resemble an MCE. To the extent that these different hypotheses are favoured by similar large-scale conditions (i.e. cyclonic horizontal shear and easterly vertical shear) it is difficult to distinguish between them on the basis of our analysis, but we can at least determine whether any of them may be consistent with the observed large-scale conditions that are favoured for the occurrence of MCEs.

We compare the large-scale conditions which are prevalent during MCEs to those which are prevalent during single TC events, and examine the difference in light of the dynamical arguments above. In doing so we test, indirectly, the hypothesis that a significant fraction of MCEs occur due to Rossby wave radiation, as well as the specific hypotheses described above about the dynamics of the radiation process. A positive result does not prove that wave radiation is dominant or that other mechanisms are not important, only that the data do not rule

out a role for wave radiation generally and the arguments of the studies cited above in particular.

2. Methods

2.1. Data sources

We use the U.S. Navy’s Joint Typhoon Warning Center (JTWC) best-track dataset for the genesis dates, locations and tracks of every TC for the period 1948–2005 in the WNP. The data is updated every six hours and comprises 1517 TCs. Genesis is defined to occur at the time and location when the storm first appears in the JTWC record. The reason that so much spatial data is presented in Figs. 5 and 6 is that long-lived cyclones that originate in the WNP occasionally head north, recurve and traverse practically the entire basin. For a few of our calculations, we track the TC for its entire lifetime, leading to a large spatial distribution of the data.

The daily winds used to estimate our shear parameter were obtained from the National Centers for Environmental Protection - The National Center for Atmospheric Research (NCEP-NCAR) reanalysis project. The horizontal wind data is gridded at each level at $2.5^\circ \times 2.5^\circ$.

2.2. Algorithms

2.2.1. Identifying MCEs. Our first task is to identify MCEs. Using only simple statistical tools, the conditions under which these events occur will then be contrasted with those under which a single TC occurs by itself.

We define an MCE as an occasion on which a second TC appears to the east of an extant one. We examine each 6 hour

time step of each of the 1517 storms’ lifecycles, and if at any point during that time another TC appears to the east of the first, we identify the first TC as the ‘mother’ and the second as the ‘daughter.’ We then move on to the next TC in the database. In the rare case when two or more TCs occur to the east at the same time in the database (‘twins’), the closest TC to the mother is called the daughter, and we move on to the next TC. By these definitions, a TC cannot be a mother more than once. We also repeated the analysis imposing a cut-off distance beyond which the two TCs were assumed unrelated (and thus not to constitute an MCE), choosing 5000 km as this distance. The frequency distributions of MCEs (discussed further below), presented with and without the cut-off distance in Fig. 1, are very similar.

2.2.2. Shear parameter U . Under the linear shallow water equations on the equatorial β -plane, the wavelength of a stationary Rossby wave in a background flow U is

$$\lambda = 2\pi R_{eq} \sqrt{\frac{1}{\frac{c}{U} - (2n + 1)}}, \tag{1}$$

where n is the meridional wave number, c is the gravity wave speed, and R_{eq} is the equatorial Rossby radius of deformation. For $U \leq 0$ or for $U \geq c/(2n + 1)$, no real solution exists to eq. (1), therefore no stationary wave train can form.

For a Rossby wave radiated by a TC in a three-dimensional flow, we interpret U as the difference between the steering flows felt by the wave and the TC. This steering flow difference can result from vertical shear, horizontal shear, or both, as discussed in the previous section.

2.2.3. Calculating the vertical shear parameter. If U in (1) is taken to represent the effect of vertical shear, then we must compute an approximate measure of vertical shear around the mother TC in order to test the hypothesis that vertical shear

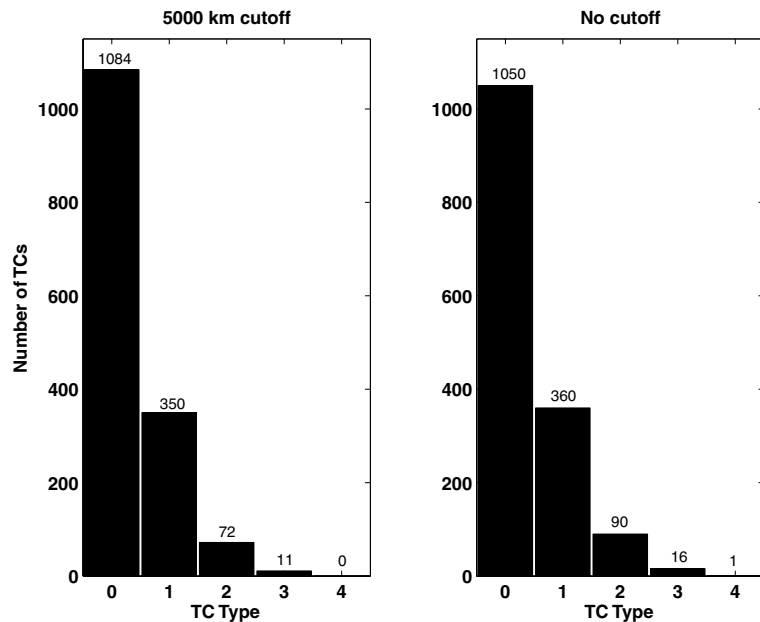


Fig. 1. Left-hand panel: the distribution of the number of TCs within 5000 km to the east of every TC in database. There are 1084 others (zero TCs to the east during TC’s lifetime), 350 events where one TC appears to the east (2 TCs within 5000 km of each other in the basin), 72 events where 2 TCs appear, 11 events where 3 TCs appear, and 0 events where 4 TCs appear. Right-hand panel: no cut-off distance: 1050, 360, 90, 16, 1.

controls Rossby wave radiation. We represent the shear by the difference between the 850 and 250 hPa zonal wind averaged over a 2500×2500 km box centred around the closest grid-point to the centre of the TC based on the JTWC record at these levels, resulting in $\langle u_{850} \rangle$ and $\langle u_{250} \rangle$, respectively, at each time step, where $\langle a \rangle$ is the spatial average of a . Then, we calculate our measure of vertical shear as $U_v = \langle u_{850} \rangle - \langle u_{250} \rangle$. Note that this differs from the conventional sign convention for vertical shear in that here easterly shear corresponds to positive U_v and westerly shear to negative U_v . Our convention is chosen for consistency with the dispersion relation, eq. (1), setting $U = U_v$.

We temporally average this shear two ways: (1) over the average time interval between the genesis of the mother and the genesis of the daughter and (2) over the entire lifetime of the mother. For all calculations presented that demonstrate average separation distances and locations, we present results from the first approach. As presented in the next section, however, the results are insensitive to this choice. Over all mother TCs, this average is called $\langle \tau_m \rangle$ and is equal to 4.5 d.

When addressing the ‘other’ TCs, U_v is calculated over both $\langle \tau_m \rangle = 4.5$ d from the date of genesis and the entire lifecycle of each other TC, as given in the JTWC dataset. Again, as presented in the next section, the main results are largely unaffected by the chosen timescale.

Because we do not have a simple way of computing the steering levels for the wave and the TC precisely, our measure of vertical shear U_v cannot be expected to correspond quantitatively to the basic flow U in eq. (1). We expect U_v to have the correct sign to represent the true difference in steering flows, and that its magnitude will be monotonically related to that of the true difference. We further expect that U_v will be greater for the mothers than for the others, as it is hypothesized that the mother TCs occur in environments of easterly shear whereas the others do not.

2.2.4. Calculating horizontal shear parameter. If U in (1) is taken to represent the effect of horizontal shear, then we must compute an approximate measure of horizontal shear around the mother TC in order to test the hypothesis that horizontal shear controls Rossby wave radiation. We compute an appropriate measure of horizontal shear by first averaging the zonal wind at 850 hPa over a rectangular region whose corners are defined by the average relative positions of the mother and the daughter TCs. As is discussed in more detail below, the average separation distance between the mother and daughter pairs is about 2400 km longitudinally and 1000 km latitudinally (the daughters, on average, spawn to the southeast of the mothers, in line with arguments and predictions). Thus we take averages over a box of 2500 km longitudinal distance by 1000 km latitudinal distance. The averaging box is located to the southeast of the mother TC. Boxes of a wide range of sizes and orientations were used (all oriented to the east of the mother), and the qualitative results were largely unaffected by this choice.

The final calculation of the horizontal shear parameter, U_h , involves the zonal steering flow of the mother TC, u_{TC} . This is assumed to be equal to the zonal motion of the TC itself. We neglect ‘beta drift’ as this gives a modest contribution to the TC motion which is largely in the meridional direction. At every 6-hour time step we calculate the average Rossby wave steering flow (which we are defining as the 850 hPa zonal flow, u_{850}) over the above-described region and arrive at $\langle u_{RW} \rangle$, and subtract the TC’s zonal velocity, so that $U_h = \langle u_{RW} \rangle - u_{TC}$. As in the vertical shear case, we temporally average over $\langle \tau_m \rangle$. We present the results from averaging over τ_m as well as over the lifecycle of the mother (what we call the ‘total track’ calculation) and show that there is little difference between the results from the two methods.

2.2.5. Calculating separation distance. The distance λ in eq. (1) is calculated as the zonal separation between the mother and daughter TCs at the time of genesis of the daughter (its first entry in the JTWC dataset). Each pair is generally not located at the same latitude, so we use the average latitude to calculate λ . Calculations using the great circle distance between the two give essentially the same results (not shown).

3. Results

3.1. Basic statistics of MCEs

There are a total of 1517 TCs in the JTWC database for the period 1948–2005. Of these, using the cut-off distance of 5000 km, we identified 433 mother/daughter pairs and 1084 others, meaning that an MCE occurred 28% of the time. (Using no maximum cut-off distance, we identified 467 mother/daughter pairs and 1050 others for an MCE frequency of 31%. By choosing to use the finite cut-off distance of 5000 km, we rejected 34 possible MCEs.) Using 8 yr of data, Ritchie and Holland (1999) found that $\cong 8\%$ of cases were formed by downstream development (synonymous with wave radiation), whereas for the 2000–2001 seasons in the WNP, Li and Fu (2006) and Fu et al. (2007) found a frequency of $\cong 18\%$. Ritchie and Holland (1999) required that the daughter occur to the southeast of the mother and form at least 72 hours after the mother. Our criteria are looser; we require only that the daughter be to the east of the mother (allowing relative motion in a cyclonic sense about the two vortices’ centre of mass to occur during the radiation process, for example, as would be expected due to mutual advection of two localized vortices) and we do not require that the mother’s formal genesis time predate the daughter’s by 72 hours (since, for example, wave radiation can occur from the mother before she reaches tropical storm intensity). These differences are presumably responsible for the larger frequency of MCE occurrence in our analysis compared to that of Ritchie and Holland (1999), Li and Fu (2006) and Fu et al. (2007) did not state precisely the criteria they used to identify their downstream development cases. Our loose criteria may well include some cases which are not actually due to downstream

development. Since wave radiation can occur in a number of large-scale settings and multiple mechanisms may be operative simultaneously, we choose to make less strict judgments at the stage of identifying MCEs.

The left panel of Fig. 1 shows the distribution of the maximum number of TCs which exist within 5000 km to the east of every TC in the JTWC database during the reference TC's lifetime. The right panel shows the distribution of TCs that develop anywhere in the basin east of the initial primary TC. For example, in the left panel there are 1084 cases where there are zero TCs that fit these criteria throughout the life of the TC. There are 350 cases where a second TC spins up within 5000 km to the east of, and within the lifetime of, another TC, etc. The results can be presented as a vector: $n_i = (1084, 350, 72, 11, 0)$ where $i = 0, 1, 2, 3, 4$. This series adds up to the total number of TCs over that period ($1084 + 350 + 72 + 11 + 0 = 1517$). The results in the right panel are $n_i = (1050, 360, 90, 16, 1)$. As expected, easing the distance restriction leads to fewer others and more mother/daughter pairs, but the distributions show small sensitivity to the choice of this distance.

The average locations of the mothers $\langle(\theta_m, \phi_m)\rangle$ and their daughters $\langle(\theta_d, \phi_d)\rangle$ (method described above) are $(20.0^\circ\text{N}, 128.0^\circ\text{E})$ and $(13.4^\circ\text{N}, 150.2^\circ\text{E})$, respectively. We determine an average other's location by tracking the others for the average lifetime of the mothers, $\langle\tau_{\text{mothers}}\rangle$, yielding $\langle(\theta_o, \phi_o)\rangle = (20.1^\circ\text{N}, 134.7^\circ\text{E})$. These average locations can be seen again in Figs. 5 and 6: the average mother's location is given by the + symbol, the average other's location by the X symbol and the average daughter's location by the O. This also gives a good impression of the size and orientation of the averaging box that we use in calculating the horizontal shear parameter for every TC.

The average daughter is located approximately 2700 km to the southeast of its mother and the average zonal separation is approximately 2400 km. This is consistent with the previous findings on easterly wave or tropical depression-type disturbances in the WNP (Reed and Recker, 1971; Nitta and Takayabu, 1985; Davidson and Hendon, 1989; Liebmann and Hendon, 1990; Lau and Lau, 1990; Takayabu and Nitta, 1993; Dunkerton and Baldwin, 1995; Sobel and Bretherton, 1999; Dickinson and Molinari, 2002; Li and Fu, 2006)

Figure 2 shows the distribution of the zonal separation distances λ for the MCEs using no cut-off distance; 467 events are shown. The insensitivity to using the 5000 km cut-off in our calculations is apparent in the figure as there are very few events that take place past 5000 km. All analyses and statistics shown below regarding MCEs are based on the data from using the 5000 km cut-off distance.

3.2. Distributions of horizontal and vertical shear for mothers and others

Figure 3 shows the results of calculating the vertical shear parameter $U_v = \langle u_{850} \rangle - \langle u_{250} \rangle$ for the independent distributions others, in the top row, and mothers, in the bottom row. The left column shows the results of calculating U_v over the entire track of each TC as it appears in the JTWC database. The right column of the others row is the calculation of U_v over, at most, the average mothers' lifetime, $\langle\tau_m\rangle = 4.5$ d; if the other TC doesn't live that long, then the calculation is over its entire lifecycle. The right column of the mothers row is the calculation of U_v over the span of time from the mother TC's genesis until the time of its daughter's genesis. This seems a reasonable approach as this is

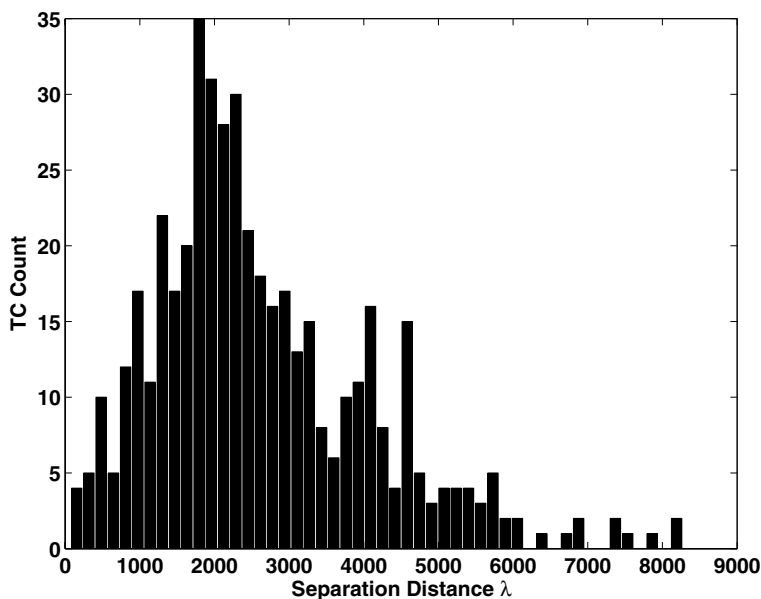


Fig. 2. The distribution of the zonal separation distances λ of MCEs using the algorithm described in the text with no cut-off distance. Note there are few events with $\lambda > 5000$ km.

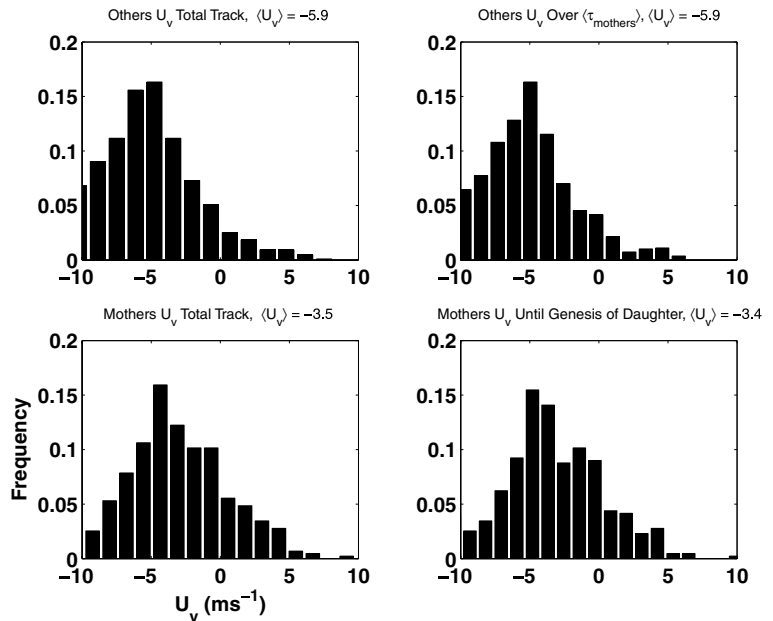


Fig. 3. Calculation of the vertical shear parameter U_v for the others, in the upper row, and mothers, in the lower row. Left column: calculation of U_v over the entire track of each TC. Right column: mothers' row is U_v until the genesis of the daughter TC, others' row is U_v over, at most, the average mother's lifetime, $\langle \tau_{mothers} \rangle$; if the other TC doesn't live that long, then the calculation is over its entire lifecycle.

most likely the span of time over which a mother storm is most strongly radiating energy to its daughter.

As can be seen in Fig. 3, in all cases the others show a pronounced shift towards more westerly shear (U_v more negative). (Remember that we have defined $U_v = \langle u_{850} \rangle - \langle u_{250} \rangle$, which is non-standard in that $U_v > 0$ means *easterly* shear ($\frac{\partial u}{\partial z} < 0$). We have defined U_v in this way for consistency with the role of U in the dispersion relation, eq. (1).)

The tendency towards more easterly shear in the mothers' versus others' distribution is in qualitative agreement with the hypothesis that MCEs should occur in regions of easterly shear. However, if vertical shear were the dominant influence on wave radiation, and U_v the appropriate measure of vertical shear, we would expect MCEs to occur only for $U_v > 0$, which is clearly not the case. There are several possible reasons for this: it could be because the hypothesis is incorrect (i.e. the properties of the stationary Rossby wave solution don't control MCE formation), because horizontal shear is more important (see below), because the mechanism might be a complicated combination of the two effects, or because U_v is not the best measure of vertical shear.

Notwithstanding the absolute signs of the two distributions, the difference between them is consistent with the hypothesis that MCEs are favoured to occur in easterly shear. The mothers' and others' distributions are significantly different at >99% confidence levels. The distributions are not normal so the standard t-test of the means might give misleading results. The so-called Wilcoxon or Mann-Whitney rank sum test is employed to arrive at the confidence levels (see, for example, Snedecor and Cochran, 1989, pp. 142-144). A Monte Carlo simulation was also carried out (using replacement) and gives the same result.

Figure 4 is oriented in the same manner as described for Fig. 3, and shows the horizontal shear parameter $U_h = \langle u_{RW} \rangle - u_{TC}$. It shows a systematically more cyclonic shear in the mothers than in the others. This, too, is in good qualitative agreement with the theory for the creation of MCEs which predicts that they should occur in cyclonic but not anticyclonic shear. This result is in fact in better quantitative agreement than the previous vertical shear results. Unlike in the vertical shear case, the absolute value of U_h of the mothers as well as the difference between the U_h distributions for mothers and others are consistent with the theory.

These distributions are significantly different at >99% confidence levels as well. The same statistical tests were performed as in the vertical shear data's case, and a Monte Carlo simulation further confirms that the distributions of the mothers and the others are indeed different.

3.3. Composites

Figure 5 shows the average difference between composites of vertical shear for mothers and the others, while Fig. 6 presents the difference in the 850 hPa zonal velocities between the same set of composites. The average locations of the mothers (+), others (X) and daughters (O) are also shown. Specifically, the calculation for Fig. 5 is

$$(\langle u_{850} \rangle - \langle u_{250} \rangle)_m - (\langle u_{850} \rangle - \langle u_{250} \rangle)_o$$

averaged over every time-step when a TC exists in the basin, for all mothers (subscript 'm') and others (subscript 'o'). It is a picture of the difference in vertical shear averaged over the days of TC activity. The figure shows that the region to the south east

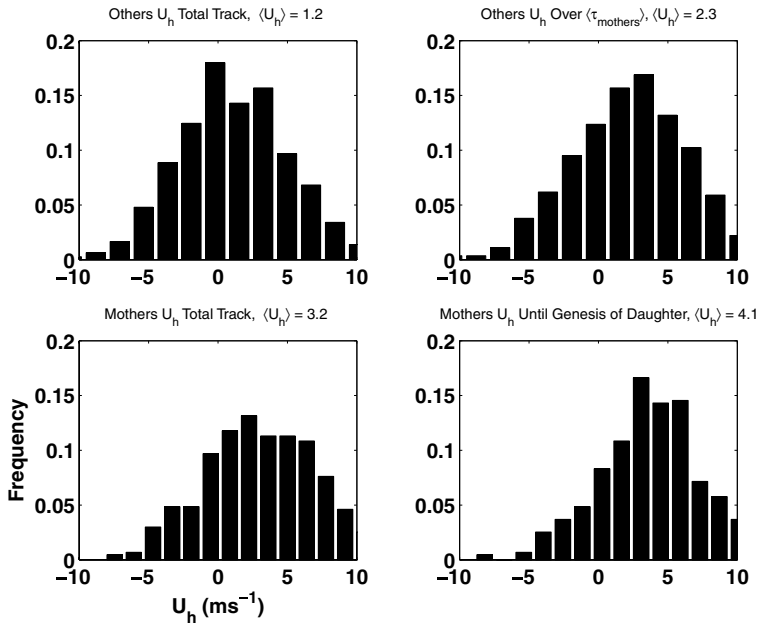


Fig. 4. Orientation of columns and rows as in Fig. 3, except here we present calculation of the horizontal shear parameter U_h .

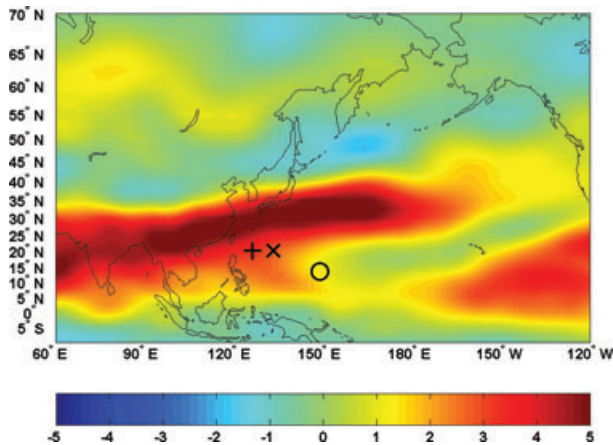


Fig. 5. The average difference in mothers' and others' vertical shear, $\langle (u_{850} - u_{250})_m \rangle - \langle (u_{850} - u_{250})_o \rangle$. The average locations of the mothers (+), others (X) and daughters (O) are shown. Notice that the region to the south east of the average mother is a region of greater easterly shear on average than that of the average other.

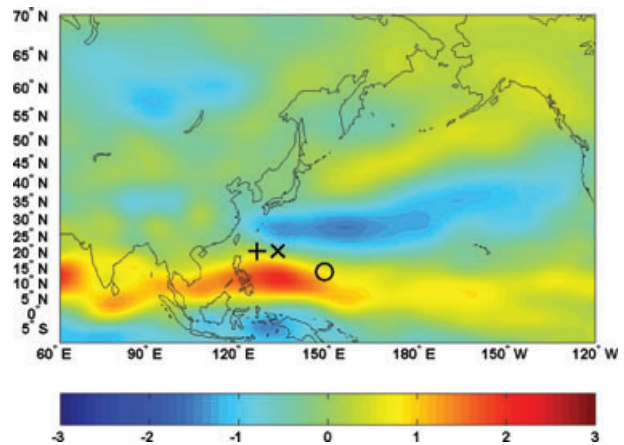


Fig. 6. The climatological difference in the mothers' and others' zonal 850 hPa flow, $\langle u_{850} \rangle_m - \langle u_{850} \rangle_o$. The average locations of the mothers (+), others (X) and daughters (O) are shown. The region bounded by the average mother and the average daughter demonstrates the low-level cyclonic shear of the flow.

of the mothers is a region of greater easterly shear on average than that region of the others. This is in accord with Fig. 4.

In Fig. 6, the calculation of the difference between mothers' and others' zonal 850 hPa flow, the temporal average is limited to the average mother's lifespan, $\langle \tau_m \rangle = 4.5$ d. If any TC doesn't live that long, then the average is taken over the lifespan of the TC. The calculation is summarized as

$$\langle u_{850} \rangle_m - \langle u_{850} \rangle_o$$

The figure shows enhanced cyclonic horizontal shear in the region around the mother and daughter in the MCE events. Some of this shear is due to the presence of the daughter itself, but its

zonal extent is greater than would be expected based on that factor alone, presumably suggesting that part of the difference is attributable to the large-scale environment rather than just to the TCs themselves.

Figure 7 presents the normalized distributions of the Julian dates of genesis of the mother and other TC types. It shows that the others' distribution is wider and that these storms, as our algorithm has chosen them, are more likely to occur in the first half of the year (the serial year, starting at January 1) than are the mother TCs. The first 100 d or so of the year show practically no mother TC activity. A rank sum test and a Monte Carlo test show that the distributions are different at >95% confidence

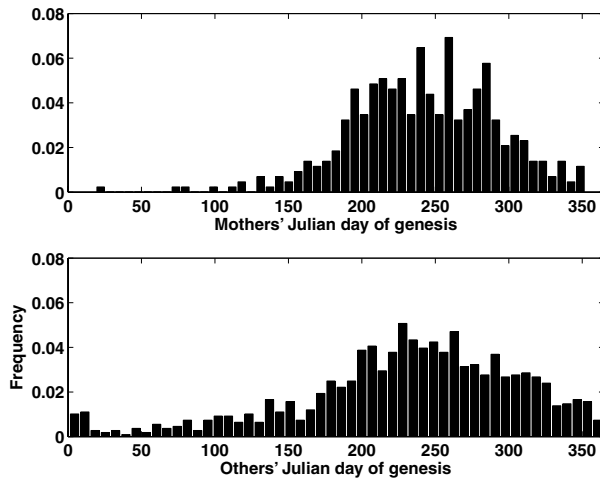


Fig. 7. Normalized distributions of the Julian (serial) dates of genesis of the mother and other TC types. They are different at >95% confidence levels.

levels. The difference is consistent with the seasonal evolution of the western north Pacific monsoon, in which easterly vertical shear and cyclonic horizontal shear, associated with monsoon deep convection, tend to develop over the western Pacific in July and decay around October and November (Murakami and Matsumoto, 1994; Wu and Wang, 2000).

3.4. Variations of MCE separation distance

The results in the previous sections address the relationship of horizontal and vertical shears to the occurrence or absence of MCEs. The occurrence of MCEs was interpreted to be a result of Rossby wave radiation from the mother TC. In Krouse et al.

(2008) we also argued that the wavelength of radiated waves, in addition the occurrence of radiation, should be controlled by shear. If this is true, there should be a relationship between the separation distance λ and one or both of the shear parameters U_v , U_h . Figure 8 is a scatterplot produced from the data presented in the lower-right panel of Fig. 4 as well as those used in Fig. 2. Each point represents a single MCE, with the zonal separation distance λ in km along the ordinate versus horizontal shear parameter U_h in ms^{-1} along the abscissa. Disregarding outliers (defined as any data greater than 2 standard deviations away from the distribution's mean, about 3% of the population), the data were then evenly binned in 50 bins in U_h . The mean of the separation data λ is represented by the X at the centre of the vertical bar, whose length is determined by the standard error of the λ data in that bin.

To the extent that λ were controlled by shear in the manner suggested by the results of Krouse et al. (2008), we should be able to fit the data to a theoretical dispersion curve. The lines show these curves, from eq. (1) for the $n = 0, 1, 2$ meridional Rossby wave modes, corresponding to the mixed Rossby-gravity (MRG) and the first two equatorial Rossby wave (ER) modes. Such a fit does not seem to explain the data particularly well. It is nonetheless encouraging to see that the majority of the data (89%) have positive U_h , as hypothesized, and that, on average, λ does increase with U_h . There is a tendency for greater variance in λ at the extremes of the range of U_h , and less variance in the central region near the intersection of the theoretical curves with the region in which most MCEs occur. While the agreement clearly could be better, it is also encouraging that the intersection occurs roughly at the average zonal separation distance of 2400 km and average value of the distribution of U_h , near $3\text{--}4 \text{ ms}^{-1}$.

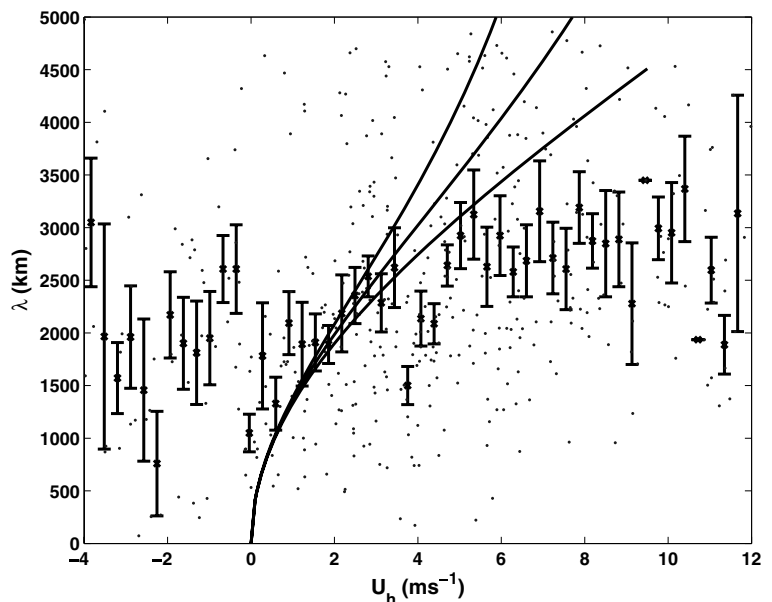


Fig. 8. Dots: individual MCEs' zonal separation distances λ versus horizontal shear parameter U_h . 89% of the λ has $U_h > 0$. Lines: centred at the mean of λ , marked with an X, length of lines is given by the standard error of the data in the bin. There are 50 bins.

In choosing the 850 hPa flow to define the horizontal shear, we are implicitly choosing 850 hPa as the Rossby wave steering level and neglecting the effects of upper level winds on the steering. As a crude sensitivity test, we have repeated the calculations using the 700 hPa in lieu of 850 hPa zonal winds in the calculation of the horizontal shear. The distributions in subsection 3.2 are little changed by this, nor is the shape of the scatterplot (not shown) corresponding to Fig. 8.

A similar scatterplot is also obtained using the vertical shear parameter U_v , except that in this case only 16% of the shear values are positive (not shown), consistent with the distributions of U_v shown above. It should be kept in mind that unlike in the case of horizontal shear, U_v is at best a qualitative proxy for the difference in the steering flows between the TC and the radiated wave. Because we do not have a simple means of computing the actual steering flows, it is not clear that the sign of U_v should correspond to the sign of the difference in the steering flows, only that we expect a more positive U_v to indicate a greater likelihood of radiation.

4. Conclusions

Using the best-track database for tropical cyclones (TCs) in the western north Pacific and the NCEP/NCAR Reanalyses, we analyzed the statistics of multiple cyclone events (MCEs). We determined the frequency of occurrence of these events, their preferred seasons of occurrence, and the large-scale conditions under which they are or are not favoured to occur. The results were interpreted in light of the hypothesis that Rossby wave radiation from the ‘mother’ TC plays an important role in the genesis of the ‘daughter’, and that that wave radiation should be favoured in the lower troposphere under large-scale cyclonic horizontal shear and easterly vertical shear. Our main findings are as follows:

(i) Defining an MCE as an event in which a daughter TC forms to the east of a mother during the mother’s lifetime, about 30% of TCs in the western north Pacific become mothers in an MCE event, with small differences in this number depending on events in which the daughter forms more than 5000 km from the mother are excluded. MCEs are relatively more likely to occur in the peak TC season and less likely to occur in the early and late season, compared to the distribution of all TCs.

(ii) Distributions of both vertical and horizontal shear in the zonal wind over the sample of MCEs compared to that of events in which a single TC did not lead to the genesis of another (‘mothers’ versus ‘others’) show that cyclonic horizontal shear at 850 hPa and easterly vertical shear are both associated with a greater likelihood of MCE occurrence.

(iii) Differences in shear, either horizontal or vertical, between one MCE and another do not seem to explain differences in horizontal wavelength according to what the linear dispersion relation would lead us to expect. However, the typical wave-

length of ~ 2000 – 3000 km (noted in many previous studies as well as this one) does seem to be crudely explained by the dispersion relation given the typical horizontal shear value of a few ms^{-1} .

5. Acknowledgments

We are indebted to Suzana Camargo for help with the best track data. We thank Suzana Camargo, Kerry Emanuel, and Tapio Schneider for discussions. This research was supported in part by NASA grant NNX07AP74A. KDK acknowledges support from the US National Science Foundation, through a Fellowship in the IGERT Joint Program in Applied Mathematics and Earth and Environmental Science at Columbia University. Insightful comments on a draft of this manuscript by Tim Dunkerton and two anonymous reviewers are appreciated.

References

- Briegel, L. and Frank, W. 1997. Large-scale influences on tropical cyclogenesis in the western north Pacific. *J. Climate* **125**, 1397–1413.
- Carr, L. and Elsberry, R. 1995. Monsoonal interactions leading to sudden tropical cyclone track changes. *Mon. Wea. Rev.* **123**, 265–289.
- Davidson, N. and Hendon, H. 1989. Downstream development in the southern Hemisphere monsoon during FGGE/WMONEX. *Mon. Wea. Rev.* **117**, 1458–1470.
- Dickinson, M. and Molinari, J. 2000. Climatology of sign reversals of the meridional potential vorticity gradient over Africa and Australia. *Mon. Wea. Rev.* **128**, 3890–3900.
- Dickinson, M. and Molinari, J. 2002. Mixed Rossby-gravity waves and western Pacific tropical cyclogenesis. Part I: synoptic evolution. *J. Atmos. Sci.* **59**, 2183–2196.
- Dunkerton, T. and Baldwin, M. 1995. Observation of 3–6 day meridional wind oscillations over the tropical Pacific, 1973–1992: Horizontal structure and propagation. *J. Atmos. Sci.* **52**, 1585–1601.
- Ferreira, R. and Schubert, W. 1997. Barotropic aspects of ITCZ breakdown. *J. Atmos. Sci.* **54**, 261–285.
- Frank, W. 1982. Large-scale characteristics of tropical cyclones. *Mon. Wea. Rev.* **110**, 572–586.
- Fu, B., Li, T., Peng, M. and Weng, F. 2007. Analysis of tropical cyclogenesis in the western north Pacific for 2000 and 2001. *Wea. Forecast.* **22**, 763–780.
- Ge, X., Li, T. and Zhou, X. 2007. Tropical cyclone energy dispersion under vertical shears. *Geophys. Res. Lett.* **34**, L23807, doi:10.1029/2007GL031867.
- Holland, G. 1995. Scale interaction in the western Pacific monsoon. *Meteor. Atmos. Phys.* **56**, 57–79.
- Krouse, K., Sobel, A. and Polvani, L. 2008. On the wavelength of the Rossby waves radiated by tropical cyclones. *J. Atmos. Sci.* **65**, 644–654.
- Lau, K.-H. and Lau, N.-C. 1990. Observed structure and propagation characteristics of tropical summertime synoptic scale disturbances. *Mon. Wea. Rev.* **118**, 1888–1913.

- Li, T. and Fu, B. 2006. Tropical cyclogenesis associated with Rossby wave energy dispersion of a preexisting typhoon. Part I: satellite data analyses. *J. Atmos. Sci.* **63**, 1377–1389.
- Li, T., Fu, B., Ge, X., Wang, B. and Ping, M. 2003. Satellite data analysis and numerical simulation of tropical cyclone formation. *Geophys. Res. Lett.* **30**, 2122–2126.
- Liebmann, B. and Hendon, H. 1990. Synoptic-scale disturbances near the equator. *J. Atmos. Sci.* **47**, 1463–1479.
- Molinari, J., Knight, D., Dickinson, M., Vollaro, D. and Skubis, S. 1997. Potential vorticity, easterly waves, and tropical cyclogenesis. *Mon. Wea. Rev.* **125**, 2699–2708.
- Murakami, T. and Matsumoto, J. 1994. Summer monsoon over the Asian continent and western north Pacific. *J. Meteor. Soc. Japan* **72**, 719–745.
- Nitta, T. and Takayabu, Y. 1985. Global analysis of the lower tropospheric disturbances in the tropics during the northern summer of the FGGE year. Part II: Regional characteristics of the disturbances. *Pure Appl. Geophys.* **123**, 272–292.
- Reed, R. and Recker, E. 1971. Structure and properties of synoptic-scale wave disturbances in the equatorial western Pacific. *J. Atmos. Sci.* **28**, 1117–1133.
- Ritchie, E. and Holland, G. 1999. Large-scale patterns associated with tropical cyclogenesis in the western Pacific. *Mon. Wea. Rev.* **127**, 2027–2043.
- Schubert, W., Ciesielski, P., Stevens, D. and Kuo, H.-C. 1991. Potential vorticity modeling of the ITCZ and the Hadley circulation. *J. Atmos. Sci.* **48**, 1493–1509.
- Shapiro, L. and Ooyama, K. 1990. Barotropic vortex evolution on a beta plane. *J. Atmos. Sci.* **170**, 170–187.
- Snedecor, G. and Cochran, W. 1989. *Statistical Methods*. 8th edn. Iowa State University Press.
- Sobel, A. and Bretherton, C. 1999. Development of synoptic-scale disturbances over the summertime tropical northwest Pacific. *J. Atmos. Sci.* **56**, 3106–3126.
- Takayabu, Y. and Nitta, T. 1993. 3-5 day period disturbances coupled with convection over the tropical Pacific ocean. *J. Meteor. Soc. Japan* **71**, 221–246.
- Wang, B. and Xie, X. 1996. Low-frequency equatorial waves in vertically sheared zonal flow: Part I: stable waves. *J. Atmos. Sci.* **53**, 449–467.
- Wang, C. and Magnusdottir, G. 2005. ITCZ Breakdown in three-dimensional flows. *J. Atmos. Sci.* **62**, 1497–1512.
- Wang, C. and Magnusdottir, G. 2006. The ITCZ in the central and eastern Pacific on synoptic time scales. *Mon. Wea. Rev.* **134**, 1405–1421.
- Wu, R. and Wang, B. 2000. Interannual variability of summer monsoon onset over the western north Pacific and the underlying processes. *J. Climate* **13**(14), 2483–2501.